

# Evaluation of forecasts by accuracy and spread in the MiKlip decadal climate prediction system

CHRISTOPHER KADOW<sup>1\*</sup>, SEBASTIAN ILLING<sup>1</sup>, OLIVER KUNST<sup>1,2</sup>, HENNING W. RUST<sup>1</sup>, HOLGER POHLMANN<sup>3</sup>, WOLFGANG A. MÜLLER<sup>3</sup> and ULRICH CUBASCH<sup>1</sup>

<sup>1</sup>Institute of Meteorology, Freie Universität Berlin, Berlin, Germany

<sup>2</sup>Zuse Institute Berlin (ZIB), Berlin, Germany

<sup>3</sup>Max-Planck-Institute for Meteorology, Hamburg, Germany

(Manuscript received July 31, 2014; in revised form April 21, 2015; accepted April 22, 2015)

## Abstract

We present the evaluation of temperature and precipitation forecasts obtained with the MiKlip decadal climate prediction system. These decadal hindcast experiments are verified with respect to the accuracy of the ensemble mean and the ensemble spread as a representative for the forecast uncertainty. The skill assessment follows the verification framework already used by the decadal prediction community, but enhanced with additional evaluation techniques like the logarithmic ensemble spread score. The core of the MiKlip system is the coupled Max Planck Institute Earth System Model. An ensemble of 10 members is initialized annually with ocean and atmosphere reanalyses of the European Centre for Medium-Range Weather Forecasts. For assessing the effect of the initialization, we compare these predictions to uninitialized climate projections with the same model system. Initialization improves the accuracy of temperature and precipitation forecasts in year 1, particularly in the Pacific region. The ensemble spread well represents the forecast uncertainty in lead year 1, except in the tropics. This estimate of prediction skill creates confidence in the respective 2014 forecasts, which depict less precipitation in the tropics and a warming almost everywhere. However, large cooling patterns appear in the Northern Hemisphere, the Pacific South America and the Southern Ocean. Forecasts for 2015 to 2022 show even warmer temperatures than for 2014, especially over the continents. The evaluation of lead years 2 to 9 for temperature shows skill globally with the exception of the eastern Pacific. The ensemble spread can again be used as an estimate of the forecast uncertainty in many regions: It improves over the tropics compared to lead year 1. Due to a reduction of the conditional bias, the decadal predictions of the initialized system gain skill in the accuracy compared to the uninitialized simulations in the lead years 2 to 9. Furthermore, we show that increasing the ensemble size improves the MiKlip decadal climate prediction system for all lead years.

**Keywords:** Decadal Prediction, Climate, Forecasts, Evaluation, Metrics

## 1 Introduction

Decadal climate prediction research gains progressively more attention in climate science as well as in society, industry and economy. The research aims to close the gap between short term forecasts and long term projections. Numerical weather predictions focus on an initial value problem in the beginning of a forecast. On the other hand, climate projections as a boundary condition problem examine the long-term development (MEEHL *et al.*, 2009; MEHTA *et al.*, 2011). In order to accommodate the demand for reliable informations on near-term climate variability on the crucial timescales of a year up to a decade, different national and international initiatives have been launched. The Coupled Model Intercomparison Project Phase 5 (CMIP5, TAYLOR *et al.*, 2012) offers a platform to approach decadal predictions on a common basis via hindcast experiments in the ‘observation’ period from 1960 to 2010.

\*Corresponding author: Christopher Kadow, Institute of Meteorology, Freie Universität Berlin, Carl-Heinrich-Becker-Weg 6–10, 12165 Berlin, Germany, e-mail: christopher.kadow@met.fu-berlin.de

The ‘Mittelfristige Klimaprognosen’ (MiKlip) project, funded by the Federal Ministry of Education and Research in Germany (BMBF), is based on CMIP5 and currently develops a decadal forecast system using the Max Planck Institute Earth System Model (MPI-ESM). With the improvements made through initialization techniques using ocean and atmosphere reanalyses in a coupled initialization (POHLMANN *et al.*, 2013), the MiKlip model version outperforms the CMIP5 complement (MÜLLER *et al.*, 2012), especially in the tropics.

In this study we present the forecasts and the skill assessment of the MiKlip decadal climate prediction system following the verification framework for interannual-to-decadal prediction experiments recommended by GODDARD *et al.* (2013). For this purpose, we employ the decadal evaluation tool ‘MurCSS’ (ILLING *et al.*, 2014) as part of the MiKlip Central Evaluation System. We point out the importance of a detailed evaluation by combining initialized decadal climate predictions with their prediction skill using the MiKlip system. In Section 2 we present the statistical methods used to evaluate the accuracy and the spread of the ensem-

ble hindcast experiment. We present decadal forecasts and their prediction skill for near surface air temperature and precipitation for lead year 1 and lead years 2 to 9, as well as the improvement due to increased ensemble size in Section 3. In Section 4, we discuss the combination of predictions and the prediction skill of the MiKlip system.

## 2 Data and methods

The MiKlip decadal forecasts and hindcasts (Baseline1, see also [POHLMANN et al., 2013](#)) used in this study were conducted with the earth system model from the Max-Planck-Institute in the low resolution version (MPI-ESM-LR). It is a coupled atmosphere-ocean system triggered by two different initialization techniques. The ocean component MPI-OM ([JUNGCLAUS et al., 2013](#)) with the resolution of  $1.5^\circ/L40$  was initialized with temperature and salinity anomaly fields from the European Centre for Medium-Range Weather Forecasts (ECMWF) ocean reanalysis system 4 ([ORAS4 – BALMASEDA et al., 2013](#)). The atmospheric component ECHAM6 ([STEVENS et al., 2013](#)) with the resolution of T63L47 was obtained by a full-field initialization with ECMWF atmosphere reanalyses, including fields of temperature, vorticity, divergence, and surface pressure (ERA40 in 1960–1989 and ERA-Interim in 1990–2013, [UPPALA et al. \(2005\)](#) and [DEE et al. \(2011\)](#) respectively). The simulations were started annually for the period 1961 to 2013, each initialization simulating a decade and consisting of 10 ensemble members.

Uninitialized runs with the same model configuration and in the same time period serve as references ([GODDARD et al., 2013](#); [MATEI et al., 2012](#)), disclosing the effect of the initialization and its potential gain of skill. The uninitialized simulations equate to the ‘historical’ experiment performed during CMIP5 using observed external forcings. Due to the fact that the ‘historical’ experiment ends in 2005, the reference run was extended by the CMIP5 ‘rcp45’ experiment consisting of the projected RCP4.5 scenario ([TAYLOR et al., 2012](#)). A 10 member experiment of uninitialized runs was conducted to have an equivalent ensemble size to the initialized runs.

We compare near surface air temperature to the HadCRUT3v ([BROHAN et al., 2006](#)) dataset from the Hadley Centre and Climatic Research Unit for the period 1961 to 2012. This commonly used anomaly data set is chosen to maintain the comparability to other decadal prediction studies ([POHLMANN et al., 2013](#); [GODDARD et al., 2013](#); [MATEI et al., 2012](#)). To enable a global comparison of precipitation with observation over land and ocean, a shorter time period was selected, focussing on the era of satellite data. The Global Precipitation Climatology Project Satellite-Gauge (GPCP-SG) dataset ([ADLER et al., 2003](#)) was used for the period from 1979 to 2012. However, for full comparability with the decadal prediction community and the evaluation over the longer

timescale, we also present the evaluation of precipitation with the Global Precipitation Climatology Centre (GPCC) Full Data Reanalysis Version 6 dataset ([SCHNEIDER et al., 2011](#); [BECKER et al., 2013](#)) over land in the supplementary material of this publication. For both evaluated variables, anomalies are considered for comparison with the model data to ensure that no general bias is influencing the results like differences in the height of model and observation.

The anomaly real-time forecasts for temperature and precipitation are available for the year 2014 and the time period of the years 2015 to 2022. The reference period is 1981 to 2010. The uninitialized simulations are used as reference datasets for the anomaly calculations.

The following skill assessment – based on the decadal climate prediction verification framework ([GODDARD et al., 2013](#)) – includes spatial averaging on a  $5 \times 5$  degree grid, temporal aggregation and lead-time dependent bias adjustment in a cross validated manner ([ICPO, 2011](#)). The lead year 1 hindcast continues the observed initial conditions in the first prediction year. For the lead years 2 to 9, the representation of the decadal-scale climate predictions excludes the skill of lead year 1. Significance of the verification scores was estimated using a non-parametric bootstrap approach ([WILKS, 2005](#); [MASON and MIMMACK, 1992](#)) taking autocorrelation into account ([GODDARD et al., 2013](#)). First, we investigate the gain of accuracy in the ensemble mean due to the initial conditions compared to uninitialized climate change projections. In a second step, we analyze whether the ensemble spread is an appropriate representation of the forecast uncertainty on average.

### 2.1 Accuracy of the ensemble mean

The mean squared error skill score (MSESS) compares the accuracy of two predictions ([MURPHY, 1988](#)) of the past, so called hindcasts. The initialized hindcasts  $H_{ij}$  consist of their ensemble members  $i = 1, \dots, m$  and the start times  $j = 1, \dots, n$ . The mean squared error (MSE) between the hindcast ensemble mean  $H_j$  and the observations  $O_j$  over  $j = 1, \dots, n$  start times can be expressed as

$$\text{MSE}_H = \frac{1}{n} \sum_{j=1}^n (H_j - O_j)^2. \quad (2.1)$$

Compared to some reference prediction, such as the climatological forecast  $\text{MSE}_{\bar{O}} = \frac{1}{n} \sum_{j=1}^n (\bar{O} - O_j)^2$ , the skill can be determined by the

$$\text{MSESS}(H, \bar{O}, O) = 1 - \frac{\text{MSE}_H}{\text{MSE}_{\bar{O}}}. \quad (2.2)$$

Applying the Murphy-Epstein decomposition and using anomalies, the MSESS for the climatological forecast

can be written as:

$$\text{MSESS}(H, \bar{O}, O) = r_{HO}^2 - \left[ r_{HO} - \frac{s_H}{s_O} \right]^2 \quad (2.3)$$

with  $r_{HO}$  being the sample correlation coefficient between the hindcasts and the observations, and the sample variance of the hindcasts  $s_H^2$  and observations  $s_O^2$  (MURPHY, 1988; MURPHY and EPSTEIN, 1989). This decomposition allows to differentiate between the correlation coefficient and the conditional prediction bias (second term on the right hand side of Eq. 2.3). When comparing the initialized hindcasts  $H$  with the uninitialized reference  $R$ , the MSESS can be written as

$$\text{MSESS}(H, R, O) = \frac{\text{MSESS}_H - \text{MSESS}_R}{1 - \text{MSESS}_R} \quad (2.4)$$

to assess the change of skill from the uninitialized to the initialized prediction system.

The MSESS represents the improvement in the accuracy of the hindcasts  $H$  over the climatology  $\bar{O}$  or a reference forecast  $R$  with respect to the observations  $O$ , where  $-\infty < \text{MSESS} \leq 1$ . A positive value suggests an improved accuracy of the hindcast ensemble mean compared to the reference, and a negative value indicates the opposite.

The correlation coefficient  $-1 \leq r \leq 1$  as the potential skill of a prediction system represents the linear relationship between a hindcast and the observation. For assessing the change in the correlation coefficient of the hindcast against a reference prediction, the difference of  $r_{HO}$  and  $r_{RO}$  is presented, with values ranging from  $-2$  to  $2$ .

The conditional bias  $-\infty < r_{HO} - \frac{s_H}{s_O} < \infty$  is the difference of the correlation and the ratio of standard deviation from a prediction and observation – it is zero at its best. The gain of the conditional bias against a reference prediction is calculated by subtracting the absolute values  $|r_{RO} - \frac{s_R}{s_O}| - |r_{HO} - \frac{s_H}{s_O}|$ . Positive values represent a decrease of bias or, in the sense of the MSESS, a gain of skill and vice versa.

## 2.2 Ensemble spread as forecast uncertainty

The spread of an ensemble forecast (ensemble variance) is meant to be an estimate of the forecast uncertainty due to uncertainty in the initial conditions. If the mean squared deviation of the observations from the ensemble mean (MSE) corresponds to the ensemble variance, the latter is a good estimate of the forecast uncertainty. Is the ensemble variance smaller than the MSE the ensemble is said to be under-dispersive (overconfident); an ensemble variance larger than the MSE indicates an over-dispersive (underconfident) ensemble. This answers the question, if the ensemble spread can be used as reference for the forecast uncertainty. Following GODDARD et al. (2013), the ensemble spread is compared to the

forecast uncertainty using a particular version of the continuous ranked probability skill score (CRPSS). The CRPSS is based on the continuous ranked probability score (MATHESON and WINKLER, 1976)

$$\text{CRPS}(H_{ij}, O_j) = \int_{-\infty}^{\infty} (F_{H_j}(y) - \mathcal{H}(y - O_j))^2 dy, \quad (2.5)$$

which integrates the squared difference between the probability distribution  $F_{H_j}$  of the ensemble forecast and the observation for a given instance  $j = 1, \dots, n$  in probability space over the predictand  $y$ . The Heaviside function  $\mathcal{H}(y - O_j)$  is the associate cumulative distribution function for the single observation. GNEITING and RAFTERY (2007) suggested to use a normal distribution with mean  $H_j$  and variance  $\sigma_H^2$  for the forecast probability density function  $F_{H_j} = \mathcal{N}(H_j, \sigma_H^2)$ . The CRPS can be expressed with the standard normal probability density and cumulative distribution function  $\varphi$  and  $\Phi$ , respectively

$$\begin{aligned} \text{CRPS}(\mathcal{N}(H_j, \sigma_H^2), O_j) = \\ \sigma_H \left[ \frac{1}{\sqrt{\pi}} - 2\varphi\left(\frac{O_j - H_j}{\sigma_H}\right) - \frac{O_j - H_j}{\sigma_H} \left( 2\Phi\left(\frac{O_j - H_j}{\sigma_H}\right) - 1 \right) \right]. \end{aligned} \quad (2.6)$$

To quantify the ensemble spread against the standard error, we use the average ensemble spread

$$\overline{\sigma_{\hat{H}}^2} = \frac{1}{n} \sum_{j=1}^n \frac{1}{m-1} \sum_{i=1}^m (\hat{H}_{ij} - \hat{H}_j)^2 \quad (2.7)$$

with the ensemble members  $\hat{H}_{ij}$  and the ensemble mean  $\hat{H}_j$  corrected for mean and conditional bias. The reference prediction has the same mean, but its variance is replaced by the MSE

$$\sigma_R^2 = \frac{1}{n-2} \sum_{j=1}^n (\hat{H}_j - O_j)^2. \quad (2.8)$$

Using these hindcast and reference distributions in the continuous ranked probability skill score for the assessment of the ensemble spread, the resulting CRPSS<sub>ES</sub> reads

$$\text{CRPSS}_{\text{ES}} = 1 - \frac{\sum_j \text{CRPS}_H(\mathcal{N}(\hat{H}_j, \overline{\sigma_{\hat{H}}^2}), O_j)}{\sum_j \text{CRPS}_R(\mathcal{N}(\hat{H}_j, \sigma_R^2), O_j)}. \quad (2.9)$$

The reference CRPSS<sub>R</sub> using the MSE represents the forecast uncertainty and thus defines the desired value for the CRPSS<sub>H</sub>, therefore CRPSS<sub>ES</sub> ≤ 0. The optimum

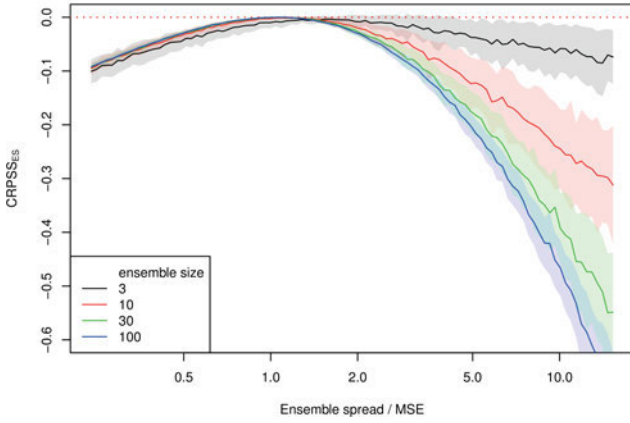


**Figure 1:** The  $CRPSS_{ES}$  as function of the ratio between ensemble spread ( $\overline{\sigma_{\hat{H}}^2}$ ) and MSE ( $\sigma_R^2$ ) for different ensemble sizes. When the given ratio is one, the  $CRPSS_{ES}$  reaches its maximum value of zero.

$CRPSS_{ES} = 0$  is attained for  $\overline{\sigma_{\hat{H}}^2} = \sigma_R^2$ , and  $\overline{\sigma_{\hat{H}}^2} \neq \sigma_R^2$  leads to a negative  $CRPSS_{ES}$ . The respective simulation study with varying ensemble size is utilized in Figure 1. This behavior does not allow to determine whether the ensemble spread is over- or underestimating the forecast uncertainty (MSE). To add this missing information, we consider the spread score (see PALMER et al., 2006; KELLER et al., 2008), with a log-transform to obtain the logarithmic ensemble spread score

$$LESS = \ln \left( \frac{\overline{\sigma_{\hat{H}}^2}}{\sigma_R^2} \right). \quad (2.10)$$

The LESS shows negative (positive) values for under-dispersive (over-dispersive) forecasts. A meaningful combination of the  $CRPSS_{ES}$  and the LESS depicts the skill and the sign of dispersion. This addresses the question whether the ensemble spread is an adequate representation of the forecast uncertainty on average posed by GODDARD et al. (2013). In this study, we define a skill score based on the LESS to compare model development stages. Different sized ensembles of the model system can be evaluated with respect to spread development.

$$LESSS = 1 - \frac{LESS_{pred}^2}{LESS_{ref}^2} \in (-\infty, 1] \quad (2.11)$$

The LESSS answers the question if the prediction system improves this ratio between the average ensemble spread and the mean squared error compared to the reference prediction.

## 3 Results

### 3.1 Forecasts and skill assessment of temperature

In general, the anomaly forecast of near surface air temperature for the year 2014 with the MiKlip system shows rather warming than cooling signals in the different regions of the world (Figure 2a). However, there are regions with strong negative and positive signals. The North-East Pacific, the western part of North America including Alaska, Central and Southern Africa as well as Russia show distinct hot spots with anomalies over 1.5 K. There are cooling patterns as well, mainly over the north-eastern North-America, India and southern China, the Antarctic Circumpolar Current and the northern North Atlantic. The forecast for the eastern Pacific points to a cooling in the ENSO region and positive anomalies in the surrounding. Over Europe, the forecast shows a warming of around 0.75 K. The climate forecast for the years 2015 to 2022 predicts a clear warming signal on the Northern Hemisphere from 60° N northwards with values over 1.5 K, beside the cooling spot in the northern North-Atlantic (Figure 3a). The forecast shows also a cooling area in the Pacific-Antarctic Basin, e.g. over the Amundsen Sea. All continents show a warming signal of around 1 K, as do the equatorial eastern Pacific, the eastern Atlantic, and the western Indian Ocean.

The analysis of the near surface air temperature in lead year 1 indicates an improvement from the uninitialized projections to the initialized hindcasts (Figure 2g,h,i). Combining the effect of increased correlation and reduced conditional bias, the MESS exhibits significant positive values over the ocean, most likely due to the ocean initialization. The North Pacific in particular benefits from the initialization (Figure 2g). The North Atlantic provides a contrast: while there is at least some improvement in correlation compared to the uninitialized runs (Figure 2h), it is accompanied by a decrease in the conditional bias (Figure 2i). The initialized hindcast experiments (Figure 2) of lead year 1 add confidence to the forecast of surface temperature in Figure 2a.

For lead years 2 to 9 (see Figure 3), the initialized and uninitialized experiments perform similarly. Due to catching the long-term trend of the climate system, the correlation coefficients for surface temperature are significantly high. Apart from the ENSO-related tropical Pacific, this is comparable to GODDARD et al. (2013) and MÜLLER et al. (2012). Little correlation is lost almost over the whole globe in the initialized runs compared to the historical runs (Figure 3h). However, small areas of positive gain in correlation can be found in the North Atlantic (Figure 3h). The conditional bias (Figure 3f) improved in the initialized runs, leading to an overall positive skill (Figure 3i). The MESS in the initialized runs against uninitialized hindcast for the surface temperature increases significantly in the tropics (Figure 3g). It decreases over areas such as northern Asia and suffers



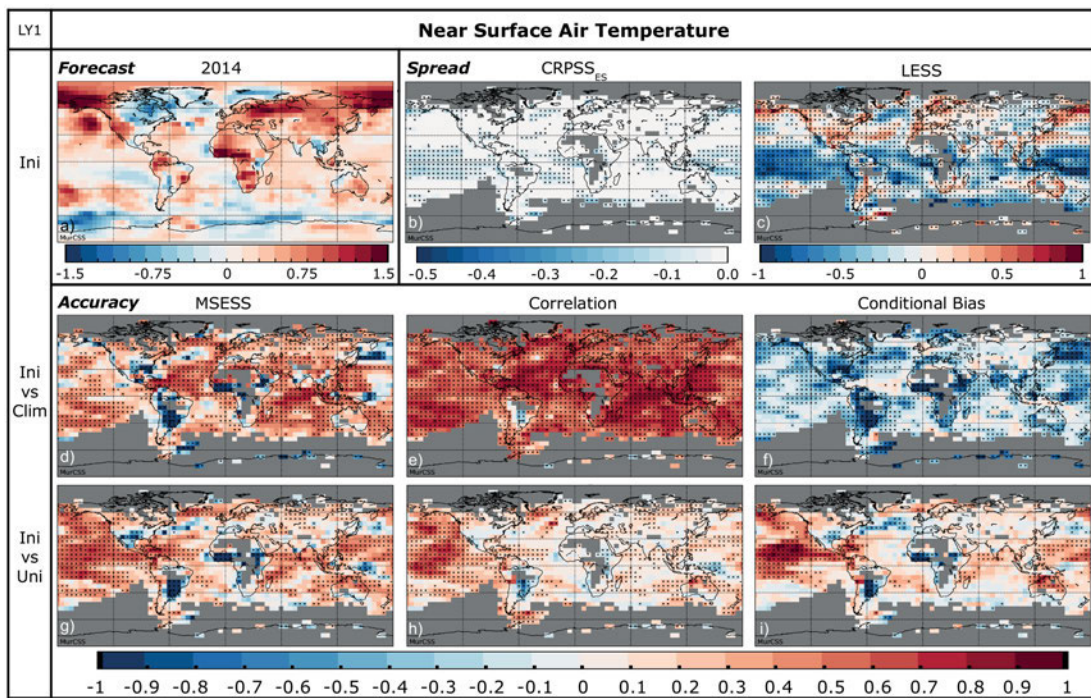


**Figure 2:** Anomaly forecast of the MiKlip decadal prediction system for near surface air temperature in Kelvin for the year 2014 (a). Anomalies are calculated relative to the years 1981 to 2010 from the uninitialized (historical and rcp45) simulations and interpolated on the  $5 \times 5^\circ$  grid for skill assessment. The evaluation of the ensemble spread is to the right of the forecast with the continuous ranked probability skill score of the ensemble spread vs the reference error (CRPSS<sub>ES</sub> in b) and the logarithmic ensemble spread score (LESS in c). The ensemble mean hindcast skill is shown in the middle and bottom row – mean squared error skill score (MSESS – left column) and its decomposition in correlation (middle column) and conditional bias (right column) of near surface air temperature averaged over the first prediction year against observation from HadCRUT3v over the period 1961–2012. It shows the skill of the initialized decadal experiments against a climatological forecast (middle row) including the MSESS (d), correlation (e) and the conditional bias (f). The lower row uses the uninitialized simulations (historical, extended with rcp45 to year 2012) as the reference prediction in the MSESS (g), the correlation differences (h) and depicting the change in magnitude of the conditional bias (i). Colorbars in the accuracy section are scaled to  $-1$  to  $1$ . Crosses denote values significantly different from zero exceeding at a 5% level applying 1000 bootstraps. Gray areas mark missing values with less than 90% data consistency in the observation.

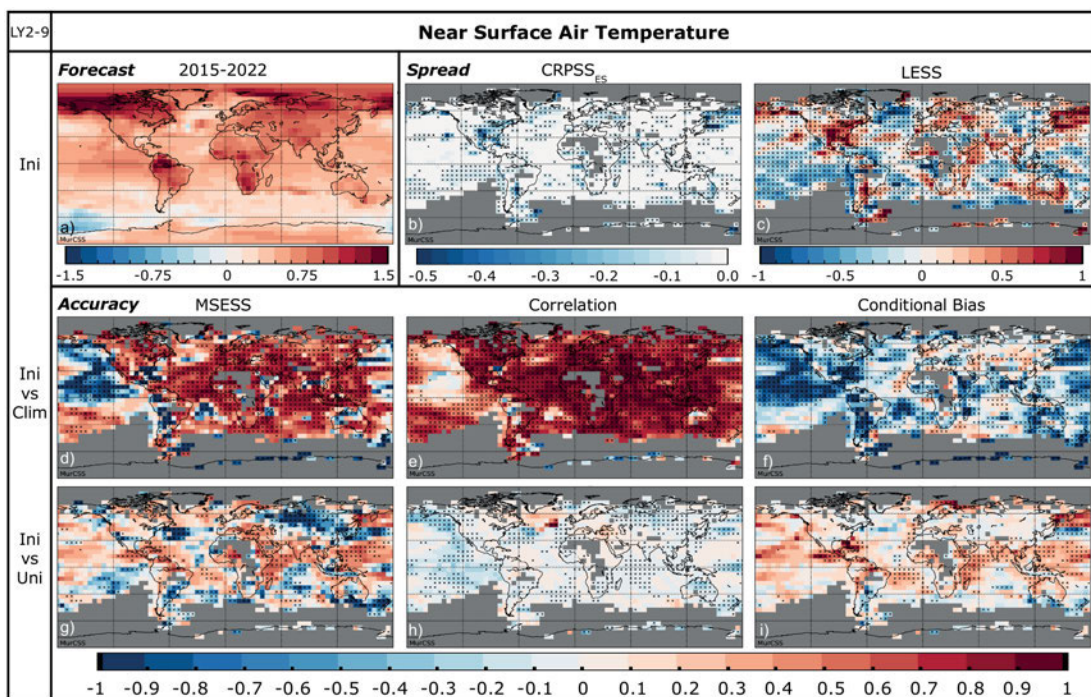


**Figure 3:** As in Figure 2 but for the forecast of 2015–2022 and evaluation of lead years 2 to 9 over the period 1962–2012.

from an increased conditional bias and negative correlation.

The CRPSS<sub>ES</sub> in Figure 2b,3b shows that the ensemble spread can represent forecast uncertainty in various regions. This is not the case in the central Pacific for lead year 1 (Figure 2b). The LESS in Figure 2c reveals that the spread is too small in the tropics and the Southern Hemisphere; this improves slightly for years 2 to 9 (Figure 3c). Variabilities around the North Atlantic as well as the North Pacific in lead year 1 (Figure 2c) show patterns with over- and under-dispersive spreads next to each other. The ensemble is over-dispersive for North America, the North Atlantic, Europe as well as around the Kuroshio, which means the ensemble spread is too large compared to the reference error (Figure 2c,3c).

The model system used in this study also participates in a multi-model comparison project as accomplished by SMITH et al. (2013). However, a different initialization strategy is applied, when comparing the real-time forecasts. The anomaly initialization in the ocean was conducted through a NCEP forced assimilation run, so called MiKlip Baseline0 simulation (see MATEI et al., 2012; MÜLLER et al., 2012). The MiKlip system as analyzed in this study (Baseline1) is closer to the multi-model average as shown in SMITH et al. (2013) than Baseline0 (not shown). In general a more uniform warming (less regions with cooling) is predicted with Baseline1 compared to Baseline0 on the longer timescales beyond lead year 1.

### 3.2 Forecasts and skill assessment of precipitation

The prediction of precipitation is more challenging, and consequently results are more dispersive than for temperature. The forecasts feature strong anomalies in the tropics and over the oceans (Figure 4a,5a). The anomaly forecast in Figure 4a shows an increase in precipitation for the year 2014 in the northern West Pacific, East Atlantic and Indian Ocean. Precipitation is decreasing in the southern equatorial Pacific and Atlantic. The forecasts over Africa and northern South America predict an overall drying, while Central America and India show a wetter signal. For the next 2 to 9 years (2015–2022) precipitation rates decrease over the northern equatorial Atlantic as well as south of the equator in the Indian Ocean and increase in the tropical Pacific. The latter shows El Niño like structures (Figure 5a). In general, the continents in the northern hemisphere show an increase, whereas the southern continents including Africa rather indicate a decrease.

The evaluation of lead year 1 shows a significant gain in correlation for the initialized over the uninitialized experiment (Figure 4h). Significant positive correlation between the decadal hindcasts and the observations from GPCP-SG (Figure 4e) is present mainly in the tropical Pacific, but can also be detected in the equatorial Atlantic and the Indian ocean. Conditional biases

for initialized (Figure 4f) and uninitialized (Figure 4i) simulations are large and negative over the whole globe compared to GPCP-SG. In the tropics in particular, the model has difficulties to reproduce precipitation variability. For the initialized run the performance is worse compared to the climatological forecast. However, the combined MSESS still shows some skill (Figure 4d,g), which can be traced back to the strong improved correlation compared to the uninitialized simulations.

The various skill scores (Figure 5) become noisy for the lead years 2 to 9. However, we present these results as well – for consistency and comparability with other international studies (GODDARD et al., 2013; SMITH et al., 2013). Some continental areas like Europe, the Middle East and North-East Asia, as well as the Indian Ocean, show some positive correlation in the decadal hindcasts compared to the climatological forecast (Figure 5e). The decadal hindcasts improve over Europe when compared to the uninitialized simulations (Figure 5h). This comes along with an improved temperature and therefore energy budget over Europe when compared to the uninitialized hindcast for the lead years 2 to 9. This gets more obvious, when the initialized system clearly outperforms the uninitialized system in the detrended temperature analysis of the MSESS and correlation in the leadyears 2 to 9 (Figure S3). This is because annual precipitation is not that trend related (KUMAR et al., 2013), especially in Europe (CUBASCH and KADOW, 2011) and the North Atlantic is shown to be the source of skill over Europe (GHOSH et al., submitted). But, due to the loss of correlation for precipitation in most of the other regions by contrast with the uninitialized runs and the negative conditional bias in the North Atlantic, as well as the same difficulties as experienced for lead year 1 at the equatorial regions in the conditional bias (Figure 5f,i), the MSESS comparison from initialization runs versus uninitialized simulations (Figure 5d,g) shows almost no skill for precipitation.

For lead year 1 the ensemble spread is an adequate estimate for the forecast uncertainty for most regions (Figure 4b). This is no longer valid for lead years 2 to 9 (Figure 5b), with only some small areas left over the ocean with the spread being close to the reference error. The CRPSS<sub>ES</sub> highlights the areas in the tropical Pacific and Atlantic showing no skill. The LESS demonstrates the over-dispersion (Figure 4c,5c) in these regions. Here, the precipitation rates suffer from positive temperature biases in the ocean in these areas (not shown), which leads to more convective activity and variability. Furthermore, the LESS reveals that areas of small and large ensemble spreads are next to each other in the central Pacific and Atlantic. This points to problems in the correct representation of small scale processes on these time scales in the spread of the ensemble. Variabilities in convective and large scale precipitation processes in climate models are difficult to represent. The standard error of satellite instruments is also relatively high in regions with little precipitation, especially in the first years of the GPCP-SG dataset (ADLER et al., 2003). The short



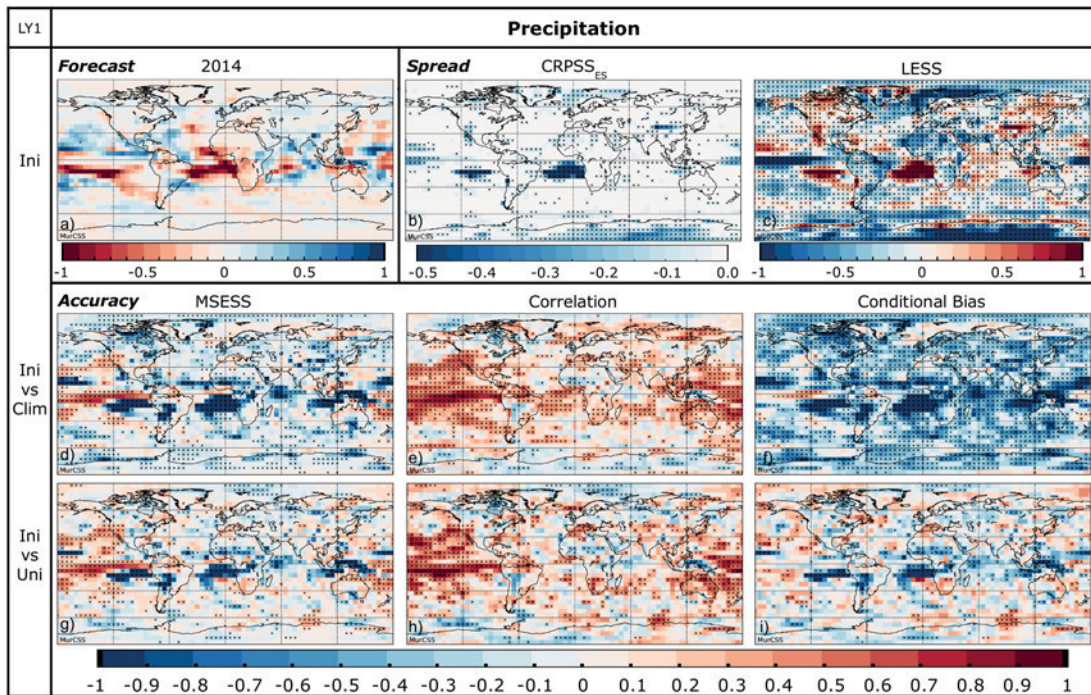


**Figure 4:** As in Figure 2 but for precipitation in mm/day and using the observation from GPCP-SG over the period 1979–2012 for skill assessment.

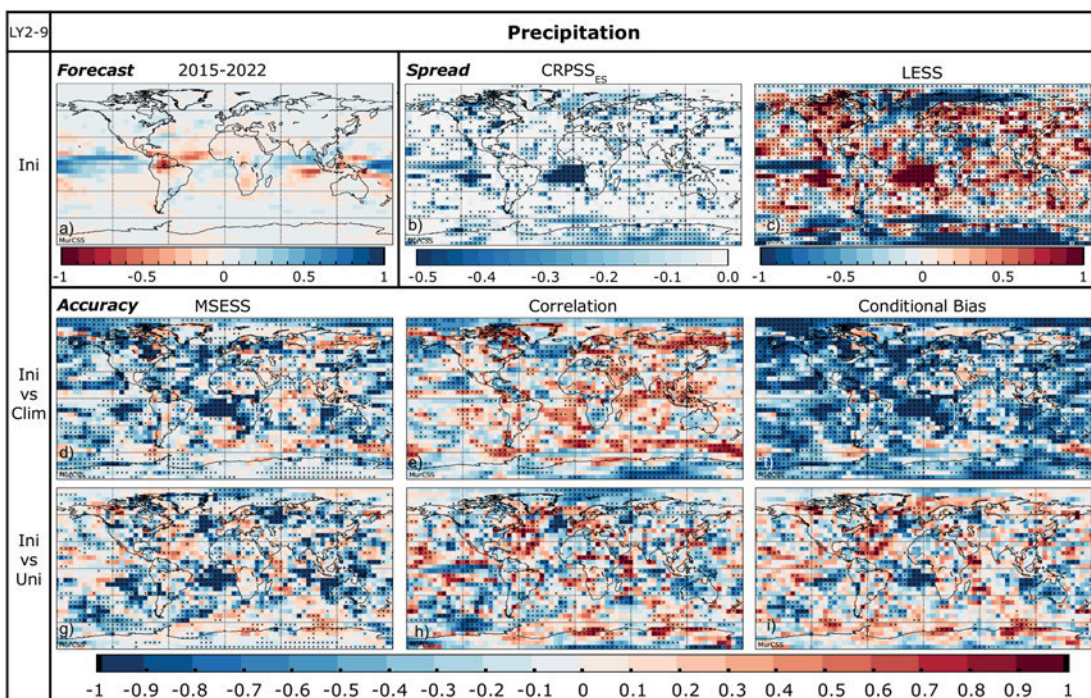


**Figure 5:** As in Figure 4 but for the lead years 2 to 9 over the period 1980–2012.

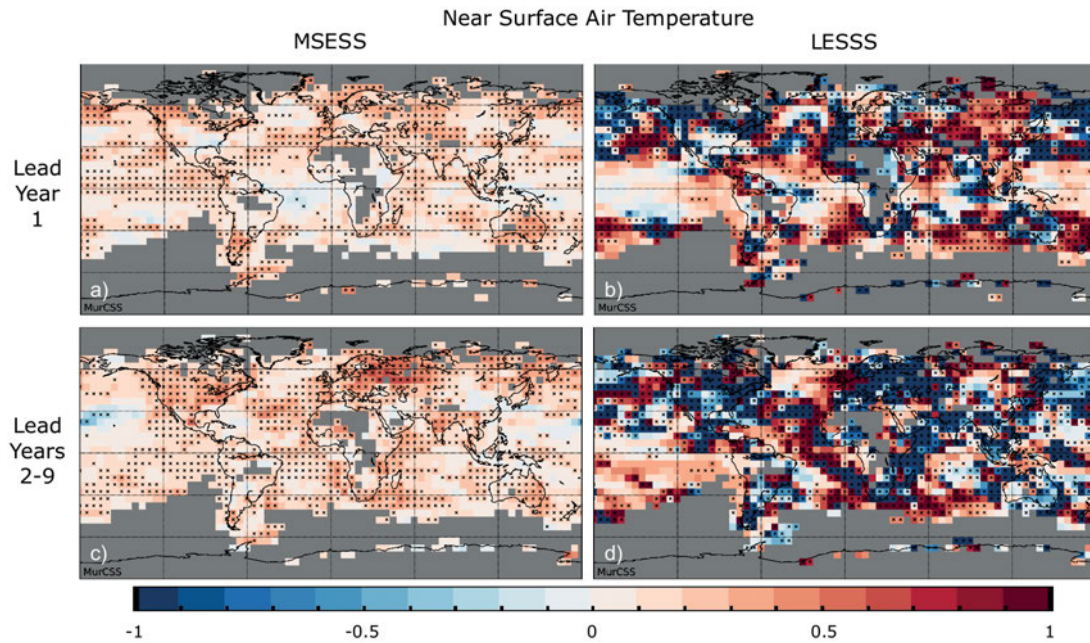


**Figure 6:** Comparison of the hindcast skill of different sized ensemble model versions (10 member vs 3 member). MSESS and LESSS for near surface air temperature over the period 1961–2012 against HadCRUT3v for the lead year 1 (upper row) and lead years 2 to 9 (lower row). The MSESS shows the improvement made in the hindcast ensemble mean prediction and the LESSS exhibit the improvement in the ensemble spread as an adequate representation of the forecast uncertainty. Crosses denote values significantly different from zero exceeding at a 5 % level applying 1000 bootstraps. Gray areas mark missing values with less than 90 % data consistency in the observation.

observational period of the satellite observations is problematic too, when analyzing the lead years 2 to 9.

### 3.3 Ensemble Size

The CMIP5 (TAYLOR et al., 2012) decadal experimental design with initializations every 5 years led to an unreliable skill assessment (GODDARD et al., 2013). Since then, most of the prediction systems are initialized annually. The small ensemble size of these experiments is another known issue, particularly for comparing different prediction systems (SMITH et al., 2013). POHLMANN et al. (2013) analyze only 3 ensemble members of the MiKlip system in order to have a clean comparison with the results of the 3 available members in the CMIP5 system. KRUSCHKE et al. (2014) use a bias corrected RPSS to compensate for different ensemble sizes. A comprehensive study on the effect of the ensemble size on decadal prediction is given in STENZ et al. (submitted). To fill the gap between the MiKlip system analyzed in POHLMANN et al. (2013) and the results shown in this study, we present the change of skill for lead years 1 and 2 to 9 by increasing the ensemble size from 3 to 10 ensemble members.

The MSESS in Figure 6 shows a significant gain of prediction skill for surface temperature. Besides the Central Atlantic, the temperature prediction skill for lead year 1 increases for the whole globe – not significant everywhere (Figure 6a). But on the long run,

the forecast for the Central Atlantic benefits from the larger ensemble for lead years 2 to 9 (Figure 6c). The LESSS for temperature shown in Figures 6b) and 6d) improves in the tropics where the CRPSS<sub>ES</sub> reveals significant negative skill (Figure 2b,3b) and the LESS (Figure 2c,3c) depicts an under-dispersion. Therefore, the decreasing under-dispersion due to the increased ensemble size leads to a slightly better representation of the uncertainty by the ensemble spread. Precipitation shows an improvement in the MSESS in lead years 1 and 2 to 9 (not shown). The LESSS improves only in local areas in the development of the ensemble spread as an adequate forecast uncertainty in the comparison of the 10 to the 3 ensemble member system for precipitation (not shown).

## 4 Discussion and conclusions

Combining forecasts and detailed evaluation for the MiKlip system for near surface air temperature and precipitation provides a comprehensive assessment of the decadal climate predictions. With a strong impact in lead year 1, initialization techniques improve the prediction system in comparison to an uninitialized system. Both atmospheric parameters benefit from an initialization with an oceanic reanalysis. Mainly the Pacific region temperature forecast improves, which causes an improved convection, triggering precipitation fluxes.



The equatorial regions suffer from an under-dispersive ensemble in temperature and an over-dispersion of precipitation in regions of western South America over the Pacific and western Central Africa over the Atlantic. Both variables exhibit a large negative conditional bias in lead year 1. The largest temperature anomalies for year 2014 are forecasted in areas where the performance of the model system is less satisfying, e.g. a warming of 3 Kelvin in West Africa or a cooling of 2 Kelvin in a small region in the North Atlantic. Regions with few data for validation like the southern Pacific can not be reliably evaluated using observational reconstructions.

As the initialized system drifts towards the same state as the uninitialized model, the lead years 2 to 9 produce similarly performances for the initialized and uninitialized experiments. The improvement of the initialized prediction system on these timescales stems from the decreased conditional bias in combination with an increased ensemble size, at least for temperature. The conditional bias exists, when a climate model e.g. over-responds to increasing greenhouse gases (GODDARD et al., 2013). This can result in an overestimation of temperature anomalies. In this respect, the initialized MiKlip prediction system performs better in the MESS than the uninitialized due to matching the climate trend much better. But it is difficult to differentiate between a model drift of the initialized system towards a warmer state of the uninitialized system and a possible predicted warming after the hiatus (MEEHL et al., 2011; KOSAKA and XIE, 2013). Analyzing a decadal prediction system being between an initial and boundary condition problem leads to several factors for potential skill. The correct initial condition in the beginning of the forecast improves the forecast on the seasonal to the interannual timescale. The memory of the ocean plays a big role on interannual to decadal timescale, when running a coupled model. But the trend due to increased greenhouse gases has even more influence on the long-term development. Analyzing the time range of 2 to 9 years mixes these potentials of skill and the uninitialized system improves on the long run. Therefore the uninitialized can outperform the initialized system in correlation like shown in this study. But, filtering the trend in the temperature hindcasts and observations showed that the initialized system beats the uninitialized simulations in terms of correlation on these timescales. However, the long-term temperature trend belongs to the 2 to 9 year forecast. This cannot be adjusted, when presenting decadal predictions.

The comparison of the 10 ensemble member system against the 3 ensemble member system (used in POHLMANN et al., 2013), shows clear improvements in the MESS over the whole globe. Even for regions of overestimated precipitation, the forecasts improved for lead years 2 to 9. The analysis of the LESS also shows a slight improvement in ensemble spread in the tropics, comparing two different ensemble sizes. In most of the regions the ensemble spread is an adequate representation for the uncertainty of this system and it is

much closer to the reference error (MSE) than for other decadal prediction systems (GODDARD et al., 2013).

Including the LESS and the LESSS to the set of skill assessment for decadal prediction allows to distinguish between an over- or under-dispersive ensemble and detect improvements made when aiming at larger ensemble sizes (SIENZ et al., submitted). The LESSS could also be used to evaluate different ensemble generation methods of the same model system to assess their possible improvement. After the development stages and accomplished improvements (MÜLLER et al., 2012; POHLMANN et al., 2013; KRUSCHKE et al., 2014; STOLZENBERGER et al., submitted; SPANGEHL et al., submitted), the next step in the ongoing MiKlip project is to switch from the anomaly initialization in the ocean with ORAS4 to full-field multi-reanalysis initialization with ORAS4 and GECCO2 (KÖHL, 2014). A first study on these combined predictions is given by KRUSCHKE et al. (submitted). The coming 30 member prediction system will allow a more robust assessment. It will be possible to involve other scores to this combined prediction system, e.g. the error spread score (CHRISTENSEN et al., 2015), which needs ensemble sizes larger than available in this study.

The decadal skill assessment used in this study is an operational part of the central evaluation in MiKlip. It is available to the climate science community (ILLING et al., 2014) and is planned to be deployed in the next stages of the MiKlip project development.

## Acknowledgments

We acknowledge funding from the Federal Ministry of Education and Research in Germany (BMBF) through the research programme MiKlip<sup>1</sup>, projects INTEGRATION (FKZ: 01LP1160A), ENSDIVAL (FKZ: 01LP1104A), and FLEXFORDEC (FKZ: 01LP1144A). We have used observational data provided by the Hadley Centre<sup>2</sup>, Global Precipitation Climatology Project<sup>3</sup>, Global Precipitation Climatology Centre<sup>4</sup> at Deutscher Wetterdienst and reanalyses from the ECMWF<sup>5</sup>. The climate simulations were performed at the German Climate Computing Centre (DKRZ<sup>6</sup>). The skill assessment is part of the Central Evaluation System<sup>7</sup> of MiKlip. The authors thank MAREIKE SCHUSTER, TIM KRUSCHKE, MADLEN FISCHER and MARTINA BALTKALNE whose comments helped to improve this paper.

<sup>1</sup><http://www.fona-miklip.de/en>

<sup>2</sup><http://www.metoffice.gov.uk/hadobs>

<sup>3</sup><http://www.gewex.org/gpcpdata.htm>

<sup>4</sup><http://gpcc.dwd.de/>

<sup>5</sup><http://www.ecmwf.int>

<sup>6</sup><https://www.dkrz.de>

<sup>7</sup><https://www-miklip.dkrz.de>

## Appendix

**Table 1:** Overview table of used variable names and equations.

Variable or Equation	Explanation
$i = 1, \dots, m$	ensemble members
$j = 1, \dots, n$	start or initialization times of experiments
$H_{ij}$	initialized hindcasts
$H_j$	ensemble mean of hindcasts
$O_j$	observations
$\text{MSE}_H = \frac{1}{n} \sum_{j=1}^n (H_j - O_j)^2$	mean squared error of the hindcast (against observation)
$\text{MSE}_{\bar{O}} = \frac{1}{n} \sum_{j=1}^n (\bar{O} - O_j)^2$	mean squared error of the climatological forecast (against observation)
$\text{ref} = \frac{A - A_{\text{ref}}}{A_{\text{perf}} - A_{\text{ref}}}$	general expression of a skill score ( $A$ value for accuracy measure, $A_{\text{perf}}$ the value for perfect prediction and $A_{\text{ref}}$ the value for a reference forecast system)
$\text{MSESS}(H, \bar{O}, O) = \frac{\text{MSE}_H - \text{MSE}_{\bar{O}}}{0 - \text{MSE}_{\bar{O}}}$ $= 1 - \frac{\text{MSE}_H}{\text{MSE}_{\bar{O}}}$	mean squared error skill score of the hindcast $H$ vs the climatological forecast $\bar{O}$ (with $\text{MSE}_{\text{perf}} = 0$ )
$\text{MSESS}(H, \bar{O}, O) = r_{HO}^2 - \left[ r_{HO} - \frac{s_H}{s_O} \right]^2$	Murphy-Epstein decomposition of the MSESS
$\text{MSESS}(H, R, O) = 1 - \frac{\text{MSE}_H}{\text{MSE}_R}$ $= \frac{\text{MSESS}_H - \text{MSESS}_R}{1 - \text{MSESS}_R}$	mean squared error skill score of the hindcast $H$ vs a reference prediction $R$
$r_{HO}$	sample correlation coefficient between hindcasts ( $H$ ) and observations ( $O$ )
$s_H^2$ and $s_O^2$	sample variance of the hindcasts and observations
$r_{HO} - \frac{s_H}{s_O}$	conditional bias of hindcasts ( $H$ ) compared to observations ( $O$ )
$\text{CRPS}(H_{ij}, O_j) = \int_{-\infty}^{\infty} (F_{H_{ij}}(y) - \mathcal{H}(y - O_j))^2 dy$	continuous ranked probability score
$\text{CRPS}(\mathcal{N}(H_j, \sigma_{H_j}^2), O_j) = \sigma_{H_j} \left[ \frac{1}{\sqrt{\pi}} - 2\varphi\left(\frac{O_j - H_j}{\sigma_{H_j}}\right) - \frac{O_j - H_j}{\sigma_{H_j}} \left( 2\phi\left(\frac{O_j - H_j}{\sigma_{H_j}}\right) - 1 \right) \right]$	continuous ranked probability score expressed with the standard normal probability density ( $\varphi$ ) and cumulative distribution function ( $\phi$ )
$\mathcal{H}(y - O_j) = \begin{cases} 1, & \text{if } y \geq O_j \\ 0, & \text{if } y < O_j \end{cases}$	Heaviside function as the associate cumulative distribution function for the single observation
$F_{H_j} = \mathcal{N}(H_j, \sigma_{H_j}^2)$	probability distribution of the ensemble forecast
$\varphi$ and $\phi$	standard normal probability density (pdf) and cumulative distribution function (cdf)
$\hat{H}_{ij}$ and $\hat{H}_j$	ensemble members and ensemble mean corrected for mean and conditional bias
$\overline{\sigma_{\hat{H}}^2} = \frac{1}{n} \sum_{j=1}^n \frac{1}{m-1} \sum_{i=1}^m (\hat{H}_{ij} - \hat{H}_j)^2$	average ensemble spread
$\sigma_R^2 = \frac{1}{n-2} \sum_{j=1}^n (\hat{H}_j - O_j)^2$	mean squared error (MSE)
$\text{CRPSS}_{\text{ES}} = 1 - \frac{\sum_j \text{CRPS}_H(\mathcal{N}(\hat{H}_j, \overline{\sigma_{\hat{H}}^2}), O_j)}{\sum_j \text{CRPS}_R(\mathcal{N}(\hat{H}_j, \sigma_R^2), O_j)}$	continuous ranked probability skill score for the assessment of the ensemble spread
$\text{LESS} = \ln\left(\frac{\overline{\sigma_{\hat{H}}^2}}{\sigma_R^2}\right)$	logarithmic ensemble spread score
$\text{LESSS} = 1 - \frac{\text{LESS}_{\text{pred}}^2}{\text{LESS}_{\text{ref}}^2} \in (-\infty, 1]$	logarithmic ensemble spread skill score



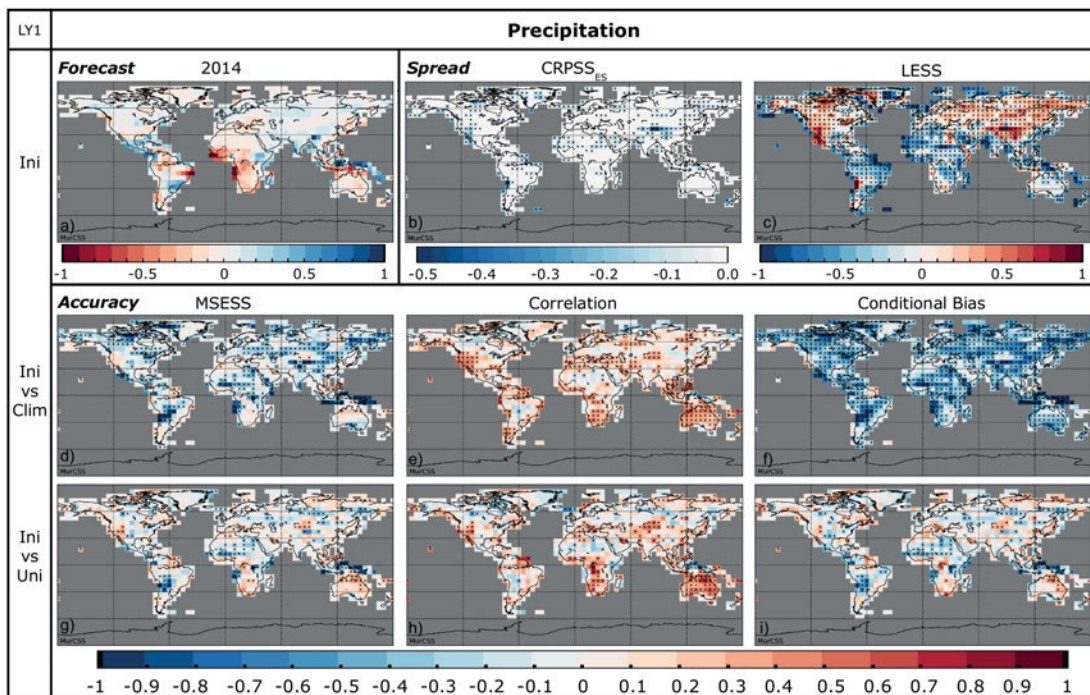


Figure S1: As in Figure 4 but using the observation from GPCC over the period 1961–2012 for skill assessment.

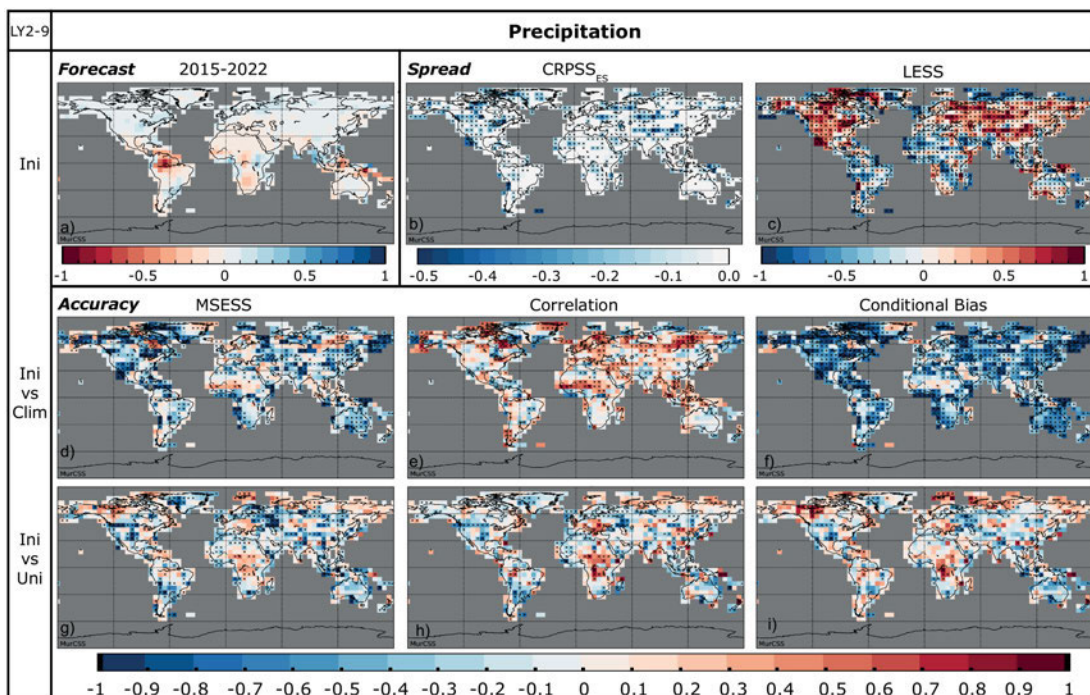


Figure S2: As in Figure 5 but using the observation from GPCC over the period 1962–2012 for skill assessment.





- KELLER, J.D., L. KORNBLUEH, A. HENSE, A. RHODIN, 2008: Towards a GME ensemble forecasting system: Ensemble initialization using the breeding technique. – *Meteorol. Z.* **17**, 707–718, DOI: [10.1127/0941-2948/2008/0333](https://doi.org/10.1127/0941-2948/2008/0333).
- KÖHL, A., 2014: Evaluation of the GECCO2 ocean synthesis: transports of volume, heat and freshwater in the Atlantic. – *Quart. J. Roy. Meteor. Soc.*, published online, DOI: [10.1002/qj.2347](https://doi.org/10.1002/qj.2347).
- KOSAKA, Y., S.-P. XIE, 2013: Recent global-warming hiatus tied to equatorial Pacific surface cooling. – *Nature* **501**, 403+, DOI: [10.1038/nature12534](https://doi.org/10.1038/nature12534).
- KRUSCHKE, T., H.W. RUST, C. KADOW, G.C. LECKEBUSCH, U. ULBRICH, 2014: Evaluating Decadal Predictions of Northern Hemispheric Cyclone Frequencies. – *Tellus A* **66**, DOI: [10.3402/tellusa.v66.22830](https://doi.org/10.3402/tellusa.v66.22830).
- KRUSCHKE, T., H.W. RUST, C. KADOW, W.A. MÜLLER, H. POHLMANN, G.C. LECKEBUSCH, U. ULBRICH, submitted: Probabilistic evaluation of Northern Hemisphere winter storm frequencies in the MiKlip decadal prediction system. – *Meteorol. Z.*
- KUMAR, S., V. MERWADE, J.L.K. III, D. NIYOGI, 2013: Evaluation of Temperature and Precipitation Trends and Long-Term Persistence in CMIP5 Twentieth-Century Climate Simulations. – *J. Climate* **26**, 4168–4185, DOI: [10.1175/JCLI-D-12-00259.1](https://doi.org/10.1175/JCLI-D-12-00259.1).
- MASON, S., G. MIMMACK, 1992: The use of bootstrap confidence-intervals for the correlation-coefficient in climatology. – *Theo. Appl. Climatol.* **45**, 229–233, DOI: [10.1007/BF00865512](https://doi.org/10.1007/BF00865512).
- MATEI, D., H. POHLMANN, J. JUNGCLAUS, W.A. MÜLLER, H. HAAK, J. MAROTZKE, 2012: Two Tales of Initializing Decadal Climate Prediction Experiments with the ECHAM5/MPI-OM Model. – *J. Climate* **25**, 8502–8523, DOI: [10.1175/JCLI-D-11-00633.1](https://doi.org/10.1175/JCLI-D-11-00633.1).
- MATHESON, J., R.L. WINKLER, 1976: Scoring Rules for Continuous Probability Distributions. – *Management Sci.* **22**, 1087–1096, DOI: [10.1287/mnsc.22.10.1087](https://doi.org/10.1287/mnsc.22.10.1087).
- MEEHL, G.A., L. GODDARD, J. MURPHY, R.J. STOUFFER, G. BOER, G. DANABASOGLU, K. DIXON, M.A. GIORGETTA, A.M. GREENE, E. HAWKINS, G. HEGERL, D. KAROLY, N. KEENLYSIDE, M. KIMOTO, B. KIRTMAN, A. NAVARRA, R. PULWARTY, D. SMITH, D. STAMMER, T. STOCKDALE, 2009: Decadal Prediction Can It Be Skillful?. – *Bull. Amer. Meteor. Soc.* **90**, 1467–1485, DOI: [10.1038/NCLIMATE1229](https://doi.org/10.1038/NCLIMATE1229).
- MEEHL, G.A., J.M. ARBLASTER, J.T. FASULLO, A. HU, K.E. TRENBERTH, 2011: Model-based evidence of deep-ocean heat uptake during surface-temperature hiatus periods. – *Nature Climate Change* **1**, 360–364, DOI: [10.1175/2009BAMS2778.1](https://doi.org/10.1175/2009BAMS2778.1).
- MEHTA, V., G. MEEHL, L. GODDARD, J. KNIGHT, A. KUMAR, M. LATIF, T. LEE, A. ROSATI, D. STAMMER, 2011: Decadal Climate Predictability And Prediction Where Are We?. – *Bull. Amer. Meteor. Soc.* **92**, 637–640, DOI: [10.1175/2010BAMS3025.1](https://doi.org/10.1175/2010BAMS3025.1).
- MURPHY, A., 1988: Skill Scores Based On The Mean-square Error And Their Relationships To The Correlation-coefficient. – *Mon. Wea. Rev.* **116**, 2417–2425, DOI: [10.1175/1520-0493\(1988\)116<2417:SSBOTM>2.0.CO;2](https://doi.org/10.1175/1520-0493(1988)116<2417:SSBOTM>2.0.CO;2).
- MURPHY, A., E. EPSTEIN, 1989: Skill Scores And Correlation-coefficients In Model Verification. – *Mon. Wea. Rev.* **117**, 572–581, DOI: [10.1175/1520-0493\(1989\)117<0572:SSACCI>2.0.CO;2](https://doi.org/10.1175/1520-0493(1989)117<0572:SSACCI>2.0.CO;2).
- MÜLLER, W.A., J. BAEHR, H. HAAK, J.H. JUNGCLAUS, J. KROEGER, D. MATEI, D. NOTZ, H. POHLMANN, J.S. VON STORCH, J. MAROTZKE, 2012: Forecast skill of multi-year seasonal means in the decadal prediction system of the Max Planck Institute for Meteorology. – *Geophys. Res. Lett.* **39**, L22707, DOI: [10.1029/2012GL053326](https://doi.org/10.1029/2012GL053326).
- PALMER, T., R. BUIZZA, R. HAGEDORN, A. LAWRENCE, M. LEUTBECHER, L. SMITH, 2006: Ensemble prediction: A pedagogical perspective. – *ECMWF Newsletter* **106**, 10–17.
- POHLMANN, H., W.A. MÜLLER, K. KULKARNI, M. KAMESWARAO, D. MATEI, F.S.E. VAMBORG, C. KADOW, S. ILLING, J. MAROTZKE, 2013: Improved forecast skill in the tropics in the new MiKlip decadal climate predictions. – *Geophys. Res. Lett.* **40**, 5798–5802, DOI: [10.1002/2013GL058051](https://doi.org/10.1002/2013GL058051).
- SCHNEIDER, U., A. BECKER, P. FINGER, A. MEYER-CHRISTOFFER, B. RUDOLF, M. ZIESE, 2011: GPCP Full Data Reanalysis Version 6.0 at 2.5: Monthly Land-Surface Precipitation from Rain-Gauges built on GTS-based and Historic Data. – Global Precipitation Climatology Centre, DOI: [10.5676/DWD\\_GPCP/FD\\_M\\_V6\\_250](https://doi.org/10.5676/DWD_GPCP/FD_M_V6_250).
- SIENZ, F., W.A. MÜLLER, H. POHLMANN, submitted: Ensemble size impact on the decadal predictive skill assessment. – *Meteorol. Z.*
- SMITH, D.M., A.A. SCAIFE, G.J. BOER, M. CAIAN, F.J. DOBLAS-REYES, V. GUEMAS, E. HAWKINS, W. HAZELEGER, L. HERMANSON, C.K. HO, M. ISHII, V. KHARIN, M. KIMOTO, B. KIRTMAN, J. LEAN, D. MATEI, W.J. MERRYFIELD, W.A. MÜLLER, H. POHLMANN, A. ROSATI, B. WOUTERS, K. WYSER, 2013: Real-time multi-model decadal climate predictions. – *Climate Dynam.* **41**, 2875–2888, DOI: [10.1007/s00382-012-1600-0](https://doi.org/10.1007/s00382-012-1600-0).
- SPANGHEHL, T., M. SCHRÖDER, S. STOLZENBERGER, R. GLOWIENKA-HENSE, A. MAZURKIEWICZ, A. HENSE, submitted: Evaluation of the MiKlip decadal prediction system using satellite based cloud products. – *Meteorol. Z.*
- STEVENS, B., M. GIORGETTA, M. ESCH, T. MAURITSEN, T. CRUEGER, S. RAST, M. SALZMANN, H. SCHMIDT, J. BADER, K. BLOCK, R. BROKOPF, I. FAST, S. KINNE, L. KORNBLUEH, U. LOHMANN, R. PINCUS, T. REICHLER, E. ROECKNER, 2013: Atmospheric component of the MPI-M Earth System Model: ECHAM6. – *J. Adv. Model. Earth Sys.* **5**, 146–172, DOI: [10.1002/jame.20015](https://doi.org/10.1002/jame.20015).
- STOLZENBERGER, S., R. GLOWIENKA-HENSE, T. SPANGHEHL, M. SCHRÖDER, A. MAZURKIEWICZ, A. HENSE, submitted: Revealing skill of the MiKliP decadal prediction systems by three dimensional probabilistic evaluation. – *Meteorol. Z.*
- TAYLOR, K.E., R.J. STOUFFER, G.A. MEEHL, 2012: An Overview Of CMIP5 And The Experiment Design. – *Bull. Amer. Meteor. Soc.* **93**, 485–498, DOI: [10.1175/BAMS-D-11-00094.1](https://doi.org/10.1175/BAMS-D-11-00094.1).
- UPPALA, S., P. KALLBERG, A. SIMMONS, U. ANDRAE, V. BECHTOLD, M. FIORINO, J. GIBSON, J. HASELER, A. HERNANDEZ, G. KELLY, X. LI, K. ONOGI, S. SAARINEN, N. SOKKA, R. ALLAN, E. ANDERSSON, K. ARPE, M. BALMASEDA, A. BELJAARS, L. VAN DE BERG, J. BIDLOT, N. BORMANN, S. CAIRES, F. CHEVALLIER, A. DETHOF, M. DRAGOSAVAC, M. FISHER, M. FUENTES, S. HAGEMANN, E. HOLM, B. HOSKINS, L. ISAKSEN, P. JANSSEN, R. JENNE, A. McNALLY, J. MAHFOUF, J. MORCRETTE, N. RAYNER, R. SAUNDERS, P. SIMON, A. STERL, K. TRENBERTH, A. UNTCH, D. VASILJEVIC, P. VITERBO, J. WOOLLEN, 2005: The ERA-40 reanalysis. – *Quart. J. Roy. Meteor. Soc.* **131**, 2961–3012, DOI: [10.1256/qj.04.176](https://doi.org/10.1256/qj.04.176).
- WILKS, D., 2005: Statistical Methods in the Atmospheric Sciences. – *International Geophysics* **100**, Academic Press, Cornell University, 627 pp.